Fractal conical lenses

Juan A. Monsoriu

Departamento de Física Aplicada, Universidad Politécnica de Valencia, Camino de Vera s/n, 46022 Valencia, Spain
jmonsori@fis.upv.es

Walter D. Furlan and Pedro Andrés

Departamento de Óptica, Universidad de Valencia, C/ Dr. Moliner 50, 46100 Burjassot, Spain

Jesus Lancis

Departamento de Ciencias Experimentales, Universitat Jaume I, Campus de Riu Sec, Ctra de Borriol, 12080 Castellón, Spain

Abstract: A conical lens is an optical element that produces a continuous focal segment along the optical axis. In this paper we introduce a more general optical device: the fractal conical lens (FCL). As the profile of a FCL is generated using the Cantor function, we show that a classical conical lens is a particular case of these fractal lenses. FCLs are distinguished by the fractal focal segments they produce along the optical axis. The influence of the Fresnel number on the axial irradiance generated by these lenses is investigated.

OCIS codes: (080.3620) Lens design; (050.1940) Diffraction; (050.1970) Diffractive optics.

References and links

1. L. M. Soroko, *Meso-Optics* (World Scientific Publishing, Singapore, 1996).
2. Z. Jaroszewicz, *Axicons, Design and Propagation Properties* (SPIE Polish Chapter Research and Development Series, Vol. 5, 1997).
3. Z. Jaroszewicz, V. Climent, V. Durán, J. Lancis, A. Kolodziejczyk, A. Burvall, and A. T. Friber, "Programmable axicon for variable inclination of the focal segment," J. Mod. Opt. **51**, 2185-2190 (2004).
4. Z. Ding, H. Ren, Y. Zhao, J. S. Nelson, and Z. Chen, "High-resolution optical coherence tomography over a large depth range with an axicon lens," Opt. Lett. **27,** 243-245 (2002).
5. Y. F. Xiao, H. H. Chu, H. E. Tsai, C. H. Lee, J. Y. Lin, J. Wang, and S. Y. Chen, "Efficient generation of extended plasma waveguides with the axicon ignitor-heater scheme," Phys. Plasmas **11**, L21-L24 (2004).
6. H. Little, C. T. A. Brown, V. Garcés-Chávez, W. Sibbett, and K. Dholakia, "Optical guiding of microscopic particles in femtosecond and continuous wave Bessel light beams," Opt. Express **12**, 2560-2565 (2004), http://www.opticsinfobase.org/abstract.cfm?URI=oe-12-11-2560
7. J. Y. L. Goh, M. G. Somekh, C. W. See, M. C. Pitter, K. A. Vere, and P. O'Shea, "Two-photon fluorescence surface wave microscopy," J. Microsc. **220**, 168-175 (2005).
8. T. Cizmár, V. Garcés-Chávez, K. Dholakia, and P. Zemánek, "Optical conveyor belt for delivery of submicron objects," Appl. Phys. Lett. **86**, 174101 (2005).
9. D. Zeng, W. P. Latham, and A. Kar, "Temperature distributions due to annular laser beam heating," J. Laser Appl. **17**, 256-262 (2005).
10. J.A. Monsoriu, C.J. Zapata-Rodríguez, and W.D. Furlan, "Fractal axicons," Opt. Commun. **263**, 1-5 (2006).
11. A.D. Jaggard and D.L. Jaggard, "Cantor ring diffractals," Opt. Commun. **158**, 141-148 (1998).
12. M.V. Pérez, C. Gómez-Reino, and J.M. Cuadrado, "Diffraction patterns and zone plates produced by thin linear axicons," Optica Acta **33**, 1161-1176 (1986).
13. J. Goodman, *Introduction to Fourier Optics* (McGraw-Hill, New York, 1996).
14. C.J. Zapata-Rodrígez and F.E. Hernández, "Focal squeeze in axicons," Opt. Commun. **254,** 3-9 (2005).
15. D.R. Chalice, "A characterization of the Cantor function," Amer. Math. Monthly **98,** 255-258 (1991).

#71609 - $15.00 USD Received 2 June 2006; revised 30 June 2006; accepted 30 June 2006

1. Introduction

The generation, manipulation, and detection of coherent conical wavefields plays a significant role in several branches of modern science and technology [1,2]. Meso-optical wavefronts are routinely generated by refractive axicons (conical lenses, CLs), reflective axicons (conical mirrors), or diffractive axicons (circular diffraction gratings). A programmable diffractive axicon has also been demonstrated by means of a commercial twisted-nematic liquid crystal display [3].

Generally speaking, an axicon can produce a narrow focal line along the optical axis (unlike the single focal point given by a spherical lens) and in a combination with a converging lens it generates a thin ring-shaped focal spot. The above features are well suited to offer optical guiding, which is the basis for much of their applications. In the past few years, conical wavefields have demonstrated its capability to maintain a lateral resolution of 10 μm over a focusing depth of 6 mm in a high-speed optical coherence tomography system [4], to generate a high-quality plasma waveguide extended to 1.2 cm for soft X-ray production [5], to guide microscopic particles in continuous wave and femtosecond light beams with a central diameter of 3-4 μm over a propagation distance of approximately 3 mm [6], to excite surface waves [7], and to trap and deliver submicron particles over a distance of hundreds of micrometers [8]. On the other hand, light structures with ring-shaped transverse cross section have a variety of applications, including laser writing and drilling [9], and material testing. For these purposes a lens-axicon system is usually applied.

Very recently, the term fractal axicon [10] has been coined to denote a Cantor ring diffractal [11] illuminated by a Bessel beam. It has been shown that the result of this combination provides a fractal on-axis intensity distribution that replicates the selfsimilar structure of the pupil. It was also suggested that fractal axicons may be useful in several applications such as optical trapping and optical metrology. The main drawback of these elements is its reduced light throughput which is inversely proportional to the level of the set of Cantor ring. This fact and the need of a special illumination beam are both limiting factors for practical applications.

This paper presents a new optical element that provides nearly the same capabilities of amplitude fractal axicons, but works under normal plane wave illumination and has a very high light gathering power. The new refractive optical element which we name *fractal conical lens* (FCL), is a CL with a Cantor-like fractal profile. In this text we study the axial irradiance provided by a FCL when illuminated with plane wavefront. In Section 2, we revise the axial behaviour of a conventional CL using the Fresnel diffraction integral and we give the practical limitation to obtain the on-axis irradiance distribution predicted by geometrical optics. In Section 3 we present the procedure we followed for the synthesis of FCL. We perform the numerical analysis of FCLs illuminated by a parallel wavefront. Additionally, the correlation between the axial irradiance provided by the FCLs and the one predicted by geometrical optics is evaluated in terms of the Fresnel number of the focusing geometry. Finally, in Section 4 the main results are outlined and some applications are proposed.

2. Axial intensity distribution of a conical lens

A CL is a glass cone made of a dielectric material with a refractive index n. A schematic representation of a CL is shown in Fig. 1(a). The transverse radius of the CL is a, and h_0 is the height. Within the paraxial regime, we consider that $a >> h_0$ (thin CL), so the base angle can be approximated to $\alpha \approx h_0/a$. When illuminated by a uniform monochromatic plane wave the CL produces a phase shift of the incident light, which decreases linearly with the radial distance r. Neglecting reflection and transmission losses, the transmission function of the CL may be written as [12]

$$T^{CL}(r) = \exp\left[-j\frac{2\pi(n-1)\alpha}{\lambda}r\right], \tag{1}$$

#71609 - $15.00 USD Received 2 June 2006; revised 30 June 2006; accepted 30 June 2006

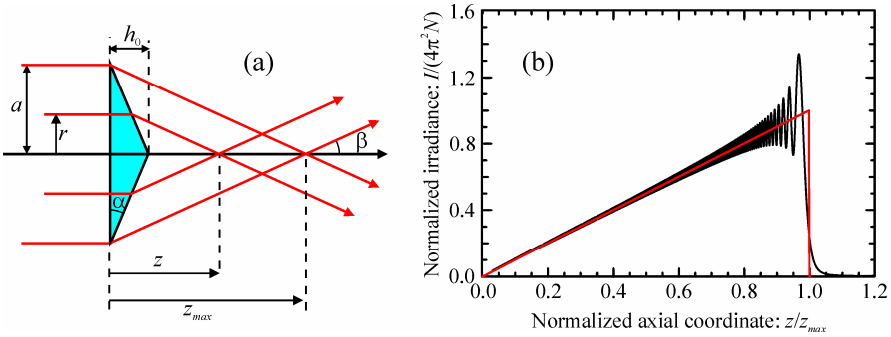

Fig. 1. (a) On-axis irradiance produced by a thin CL. The transverse radius of this axicon is a, h_0 is the height, and α is the base angle. (b) Normalized axial irradiances given by a conventional CL for N=700, and the color lines correspond to a focusing geometry of an ideally infinite Fresnel number.

where λ is the wavelength of the incident light. The parameter α determines the inclination of the beam, $\beta = (n-1)\alpha$, with respect to the optical axis, of the conical wavefront leaving the CL. Consequently, the CL produces a continuos focus line of length $z_{max} \approx a/\beta$.

According to the Fresnel-Kirchoff difracction integral [13], the on-axis irradiance distribution of a CL illuminated by a plane wave is given by

$$I^{CL}(z) = \left(\frac{2\pi}{\lambda z}\right)^2 \left| \int_0^a \exp\left[-j\frac{2\pi(n-1)\alpha}{\lambda} r\right] \exp\left[j\frac{\pi}{\lambda z} r^2\right] r\, dr \right|^2 . \qquad (2)$$

For our purposes it is convenient to express the previous integral as function of a normalized radial coordinate, $\rho = r/a$, and a normalized axial coordinate, $\bar{z} = z/z_{max}$. The result is:

$$I^{CL}(\bar{z}, N) = \left(\frac{2\pi N}{\bar{z}}\right)^2 \left| \int_0^1 \exp[-j2\pi N\rho] \exp\left[j\frac{\pi N}{\bar{z}}\rho^2\right] \rho\, d\rho \right|^2 , \qquad (3)$$

where we have introduced the Fresnel number, $N=a\beta/\lambda$ [14]. Note that N is the only parameter that appear in Eq. (3) apart from the normalized axial coordinate, and therefore, it characterizes the focusing properties of the CL. For finite Fresnel numbers the theory predicts a lineary increasing axial irradiance modulated by a rapidly oscillating pattern with growing amplitude along the axial coordinate, up to $z=z_{max}$ [see Fig. 1(b)]. This modulation also depends on N [14]. For a high Fresnel numbers it is easy to obtain that the on-axis irradiance distribution tends to

$$I^{CL}(\bar{z}, N \to \infty) = (2\pi)^2 N\, \bar{z}\, \mathrm{rect}[\bar{z} - 0.5], \qquad (4)$$

where rect(x) = 1 for $|x|<1/2$ and 0 otherwise. Therefore, in this case the on axis irradiance increases linearly, up to the geometrical shadow boundary defined by z_{max}. Out of this region the irradiance vanishes [see the red line in Fig. 1(b)]. Next we focus our attention to the FCLs.

3. Cantor-like fractal conical lenses

We define a FCL as a rotationally symmetric lens that is generated from a 1D Cantor set as follows. We start by constructing a 1D fractal pattern as for example the triadic Cantor set shown in the upper part of Fig. 2(a). The first step in the construction procedure consists in defining a straight-line segment of unit length called *initiator* (stage S=0). Next, at stage S=1, the *generator* of the set is constructed by dividing the segment in three equal parts of length

#71609 - $15.00 USD Received 2 June 2006; revised 30 June 2006; accepted 30 June 2006

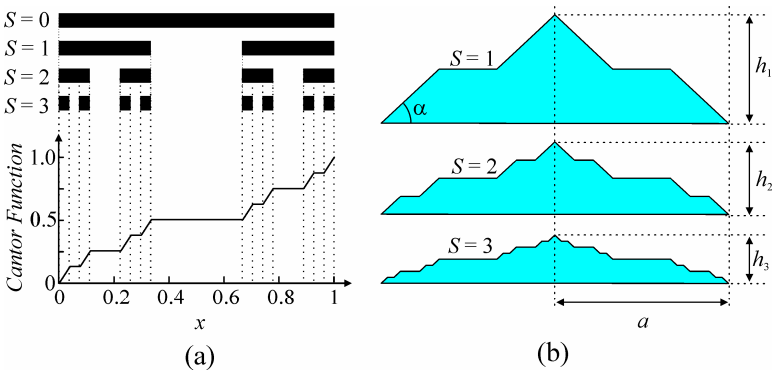

Fig. 2. (a) Triadic Cantor set for S=1, S=2, and S=3. The structure for S=0 is the initiator and the one corresponding to S=1 is the generator. The Cantor function F_S(x) is shown under the corresponding Cantor set for S=3. (b) FCLs at stages of growth S=1, S=2, and S=3.

1/3 and removing the central one. Following this procedure in subsequent stages S=2, 3, … is easy to see that, in general, at stage S there are 2^S segments of length 3^{-S} with 2^S–1 disjoint gaps located at the intervals $[p_{S,l}, q_{S,l}]$, with l=1, …, 2^S–1. For example, for S=2, the triadic Cantor set presents three gaps at [1/9, 2/9], [3/9, 6/9], and [7/9, 8/9]. In Fig. 2(a), only the three first stages are shown for clarity.

Based on the Cantor set, the Cantor function [15], $F_S(x)$, is defined in the interval [0, 1] as,

$$F_S(x)=\begin{cases}\dfrac{l}{2^S} & \text{if} \quad p_{S,l}\le x\le q_{S,l}\\ \dfrac{1}{2^S}\dfrac{x-q_{S,l}}{p_{S,l+1}-q_{S,l}}+\dfrac{l}{2^S} & \text{if} \quad q_{S,l}\le x\le p_{S,l+1}\end{cases}, \tag{6}$$

with l=1, …, 2^S–1. The lower part of Fig. 2(a) shows the Cantor function $F_3(x)$. On the intervals [1/27, 2/27], [3/27, 6/27], [7/27, 8/27], [9/27, 18/27], [19/27, 20/27], [21/27, 24/27], and [25/27, 26/27], the constant values of $F_3(x)$ are 1/8, 2/8, 3/8, 4/8, 5/8, 6/8, and 7/8, respectively. Outside of these intervals, $F_S(x)$ is a continuous increasing linear function.

We define a FCL as a circularly symmetric lens with a profile which follows the Cantor function at a given stage, S. In order to maintain a constant value of the base angle, α, at different stages S, the height of the triadic FCL is $h_S = (2/3)^S h_0$, where h_0 is the height of a FCL at S=0 corresponding to the conventional CL. Figure 2(b) shows FCLs generated for different values of S. Note that a FCL can be constructed by combining certain sections of a conventional CL. In mathematical terms, a FCL developed up to a certain growing stage S, can be represented by a phase transmission function given by,

$$T^{FCL}(\rho,N,S)=\exp\left[-j2\pi N\left(\frac{2}{3}\right)^S F_S(\rho)\right]. \tag{7}$$

When S=0 Eq. (7) reduces to Eq. (1). Therefore, we have developed a theoretical framework for the FCL in which the classical CL is a particular case.

Using the same approach as in Section 2, the irradiance distribution along the optical axis can be now written as

$$I^{FCL}(\bar{z},N,S)=\left(\frac{2\pi N}{\bar{z}}\right)^2\left|\int_0^1 T^{FCL}(\rho,N,S)\exp\left[j\frac{\pi N}{\bar{z}}\rho^2\right]\rho\,d\rho\right|^2. \tag{8}$$

#71609 - $15.00 USD Received 2 June 2006; revised 30 June 2006; accepted 30 June 2006

The axial irradiance in the region of interest was computed using the above equations for the FCLs with the values S=1, 2, and 3. The results for a Fresnel number N=700 are shown in Fig. 3 (black lines). The first noticeable feature in these figures is that the axial irradiances increases with distance z, as happens with conventional CL, but in this case it is modulated by the corresponding Cantor set. In other words, the axial irradiance reflects the fractal structure that the lenses has along the radial coordinate. It is important to note that the axial irradiance for a given stage S is a scaled and replicated version of the axial irradiance for the previous stage, as corresponds to a self-similar structure.

If we use the geometrical approximation, assuming a very high Fresnel number, we found

$$I^{FCL}\left(\bar{z},N\to\infty,S\right)=\left(2\pi\right)^2 N\,\bar{z}\prod_{i=0}^{S} g\left(\bar{z},2/3^i\right), \tag{9}$$

where $g(x,\Lambda)$ is a Ronchi-type periodic binary function with period Λ that can be written as

$$g\left(x,\Lambda\right)=\mathrm{rect}\left(x\text{-}0.5\right)\mathrm{rect}\left[\mathrm{mod}\left(x+0.5\Lambda-1,\Lambda\right)/\Lambda\right]. \tag{10}$$

In this equation mod(u,v) gives the remainder on division of u by v. Fig. 3 also shows (color lines) the axial irradiances produced by the FCLs under the geometrical approximation [Eq. (9)].

To investigate quantitatively the influence of the Fresnel numbers on the axial response of FCLs when illuminated by a plane wave, we use a correlation coefficient between the axial irradiance provided by theses lenses [Eq. (8)] and the corresponding irradiance predicted by geometrical optics [Eq. (9)], i.e.,

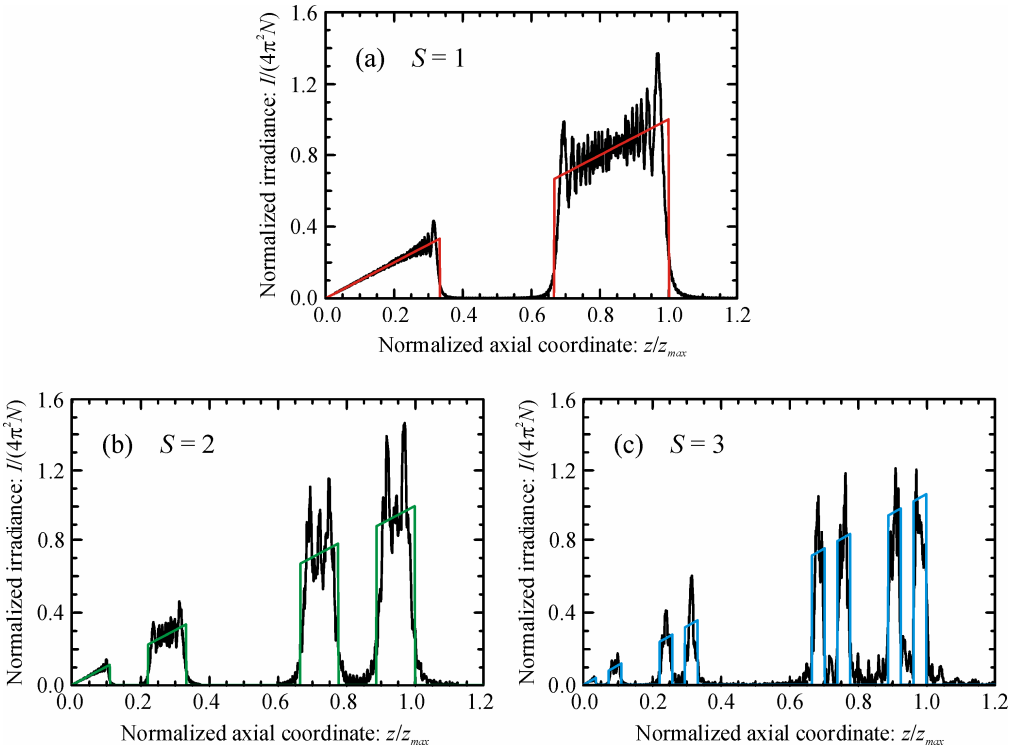

Fig. 3. Normalized axial irradiances given by FCLs for (a) S=1, (b) S=2, and S=3. Solid lines correspond to the case N=700, and the color lines correspond to a focusing geometry of an ideally infinite Fresnel number.

#71609 - $15.00 USD Received 2 June 2006; revised 30 June 2006; accepted 30 June 2006

$$C_S(N)=\frac{\int_0^{\infty} I^{FCL}(\bar{z},N,S)I^{FCL}(\bar{z},N\to\infty,S)d\bar{z}}{\int_0^{\infty}\left[I^{FCL}(\bar{z},N\to\infty,S)\right]^2 d\bar{z}}. \tag{11}$$

Using the above definition the accuracy of the geometrical approximation can be numerically evaluated. Fig 4 shows the correlation function $C_S(N)$ for different values of S. Compared with the result obtained for S=1 (red line) the correlation function for increasing fractal level of growth gives lower values. However, in all cases the correlation coefficient is an increasing function which tends to the unity for very high Fresnel number. Note that some oscillations appears for higher values of S which are the result of the lobes in the axial irradiance patters.

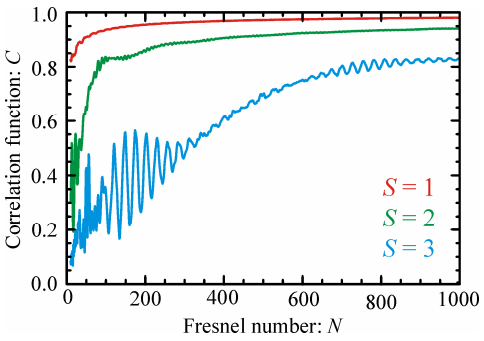

Fig. 4. Correlation function $C(N)$ between the axial irradiance given by a FCL at different stage of growth, S, and the corresponding irradiance with an ideally infinite Fresnel number.

4. Conclusions

The FCL, a new type of CL having a fractal profile based on the Cantor function has been introduced. The design of these lenses is described and the expressions for the construction parameters are derived. It is shown that a given FCL can be realized as a conventional CL in which some sections have been eliminated. Furthermore, from a theoretical point of view, a FCL can be understood as a generalization of a CL since its transmittance function is obtained as a particular case of Eq. (7) when S=0. The axial irradiance provided by FCLs illuminated by a monochromatic wavefront has been investigated. We have shown that these lenses produces focal segments distributed along the optical axis in a way that they reproduce the fractal profile of the originating FCL.

It is worth to mention that a diffractive FCL can be designed following the same approach illustrated in Fig. 2(b), by defining a surface-relief that matches a phase profile constructed by 2π phase differences between the different steps in the Cantor function and constant zero phase in the gaps of the Cantor set.

Several potential applications of FCL arise especially in scientific and technological areas where conventional CL have been successfully applied (such as metrological applications or optical trapping). In particular, the non-uniform distribution of the fractal focal segment along the optical axis could be exploited in the alignment of optical systems and mechanical devices.

Acknowledgments

The authors whish to express their gratitude to C.J. Zapata-Rodríguez for stimulating conversations. This research has been supported by the Plan Nacional I+D+i (grant DPI2003-04698), Ministerio de Ciencia y Tecnología, Spain. We also acknowledge the financial support from the Universidad Politécnica de Valencia (Vicerrectorado de Innovación y Desarrollo, Programa de Incentivo a la Investigación de la UPV 2005), Spain. J.L. also acknowledges financial support from the Plan Nacional I+D+i (grant FIS2004-02404).